

1 **A multi-proxy assessment of terrace formation in the lower Trinity** 2 **River valley, Texas**

3

4 Hima J. Hassenruck-Gudipati¹, Thaddeus Ellis¹, Timothy A. Goudge¹, David Mohrig¹

5 ¹Department of Geosciences, Jackson School of Geosciences, The University of Texas at Austin, Austin, 78712, USA

6 *Correspondence to:* Hima J. Hassenruck-Gudipati (himahg@utexas.edu)

7 **Abstract.** A proposed null hypothesis for fluvial terrace formation is that internally generated or autogenic processes such as
8 lateral migration and river-bend cutoff produce variabilities in channel incision that lead to the abandonment of floodplain
9 segments as terraces. Alternatively, fluvial terraces have the potential to record past environmental changes from external
10 forcings that include temporal changes in sea-level and hydroclimate. Terraces in the Trinity River valley have been previously
11 characterized as Deweyville groups and interpreted to record episodic cut and fill during late Pleistocene sea-level variations.
12 Our study uses high-resolution topography of a bare-earth digital elevation model derived from airborne lidar surveys along
13 ~88 linear km of the modern river valley. We measure both differences in terrace elevations and widths of paleo-channels
14 preserved on these terraces in order to have two independent constraints on terrace formation mechanisms. For 52 distinct
15 terraces, we quantify whether there is a clustering of terrace elevations – expected for allogenic terrace formation tied to
16 punctuated sea-level and/or hydroclimate change – by comparing variability in a grouped set of Deweyville terrace elevations
17 against variability associated with randomly selected terrace sets. Results show Deweyville groups record an initial valley
18 floor abandoning driven by allogenic forcing, which transitions into autogenic forcing for the formation of younger terraces.
19 For these different terrace sets, the slope amongst different terraces stays constant. For 79 paleo-channel segments preserved
20 on these terraces, we connected observed changes in paleo-channel widths to estimates for river paleo-hydrology over time.
21 Our measurements suggest the discharge of the Trinity River increased systematically by a factor of ~2 during the late
22 Pleistocene. Despite this evidence of increased discharge, the similar down-valley slopes between terrace sets indicate that
23 there were likely no increases in sediment-to-water discharge ratios that could be linked to allogenic terrace formation. This is
24 consistent with our elevation clustering analysis that suggests younger terraces are indistinguishable in their elevation variance
25 from autogenic terrace formation mechanisms, even if the changing paleo-channel dimensions might, viewed in isolation,
26 provide a mechanism for allogenic terrace formation. Methods introduced here combine river-reach scale observations of
27 terrace sets and paleohydrology with local observations of terraces and paleo-channels to show how interpretations of allogenic
28 versus autogenic terrace formation can be evaluated within a single river system.

29 **1 Introduction**

30 River valleys commonly contain fluvial terraces representing segments of older floodplain that are now located at
31 elevations distinctly above the modern floodplain. These terraces sometimes preserve paleo-channels, or remnant river-channel
32 segments. For exceptionally preserved features, channel widths, depths, bend amplitudes and wavelengths, and grain size
33 record a signal of past river hydrology. Terrace formation requires net river incision that can be allogenicly driven by tectonic
34 uplift, sea-level fall, and/or modifications to water and sediment discharge via climate change or land-use change, including
35 dam construction (Bull, 1990; Hancock and Anderson, 2002; Mackey et al., 2011; Pazzaglia, 2013; Womack and Schumm,
36 1977). What is more controversial is the character of the trigger that leads to the relatively discrete transfer of a section of
37 active floodplain or valley floor into an inactive terrace or set of terraces elevated above flood height. In particular, can terraces
38 formed by a punctuated sea-level fall, tectonic uplift, or sediment-to-water flux change be accurately separated from terraces
39 formed by lateral migration and incision connected with the autogenic processes of river channel migration and channel-bend
40 cutoff? Here we use attributes of terraces and their preserved paleo-channels in the coastal Trinity River valley in order to
41 evaluate the likelihood of allogenic versus autogenic triggers driving terrace formation for previously established groups of
42 Deweyville terraces (Bernard, 1950; Blum et al., 1995). Understanding how these terraces were most likely formed will help
43 to constrain interpretations of the input signals for downstream deltaic deposits, which are recognized to embed both allogenic
44 and autogenic signals (Guerit et al., 2020).

45 Commonly invoked allogenic triggers connected with terrace formation are punctuated decreases in sediment-to-
46 water flux that are assumed to embed a signal of regional climate change and punctuated base-level fall controlled by either
47 sea-level fall or tectonic uplift, all of which can drive periods of increased vertical incision along an extended length of river
48 channel (Blum et al., 1995; Blum and Törnqvist, 2000; Bull, 1990; Daley and Cohen, 2018; Hancock and Anderson, 2002;
49 Merritts et al., 1994; Pazzaglia, 2013; Pazzaglia and Gardner, 1993; Rodriguez et al., 2005; Wegmann and Pazzaglia, 2002).
50 These focused periods of downcutting are interpreted to produce a spatially extensive terrace, or set of terraces, that preserve
51 a fraction of the active fluvial surface and its river channel at the time of the terrace-forming event (Bull, 1990; Molnar et al.,
52 1994; Pazzaglia, 2013; Pazzaglia et al., 1998). One expected morphology for terraces formed by allogenic triggers are extensive
53 terraces flanking both sides of the river at a similar elevation, which would be expected during synchronous river incision.
54 However, it is important to realize that the extent and pairing of these terraces can be substantially modified during ongoing
55 valley incision and that unequal channel migration during relatively slow incision rates can produce similar characteristics
56 (Limaye and Lamb, 2016; Malatesta et al., 2017).

57 Both theory (Parker et al., 1998a; Wickert and Schildgen, 2019) and experiments (Tofelde et al., 2019; Whipple et
58 al., 1998) have shown how the long profile of a fluvial valley is set by the ratio of sediment-to-water discharge. Decreases in
59 water-to-sediment flux led to slope increases via alluviation. Conversely, increases in water-to-sediment flux produce lower
60 slopes through channel incision and valley formation. An allogenic trigger for terrace formation associated with
61 paleohydrology change is therefore expected to produce a long profile for older terraces that are steeper than the long profile

62 of the younger and incising river. This reduction from the measured paleo-slopes of terrace sets to the modern channel has
63 been observed in both natural (Poisson and Avouas, 2004) and experimental (Tofelde et al., 2019) systems. Interestingly, a
64 change in climate that produced similar decreases or increases in both the water and sediment discharges would yield no change
65 in the downstream slope of the system and no episode of incision to drive terrace formation. Since water and sediment
66 discharges are strongly correlated within fluvial systems (Blom et al., 2017; Lane, 1955), it is quite possible that climate change
67 might not provide an allogenic trigger for terrace formation. If long profiles extracted from terrace sets are parallel to the slope
68 of the modern river than a different driver of incision must be at work. In the greater coastal zone this can be a base-level drop
69 tied to sea-level fall (Tofelde et al., 2019). For this reason it is tempting to use interpreted sets of subparallel terraces as a proxy
70 record for fluctuations in sea-level through time (Blum et al., 1995; Blum and Törnqvist, 2000; Merritts et al., 1994; Rodriguez
71 et al., 2005).

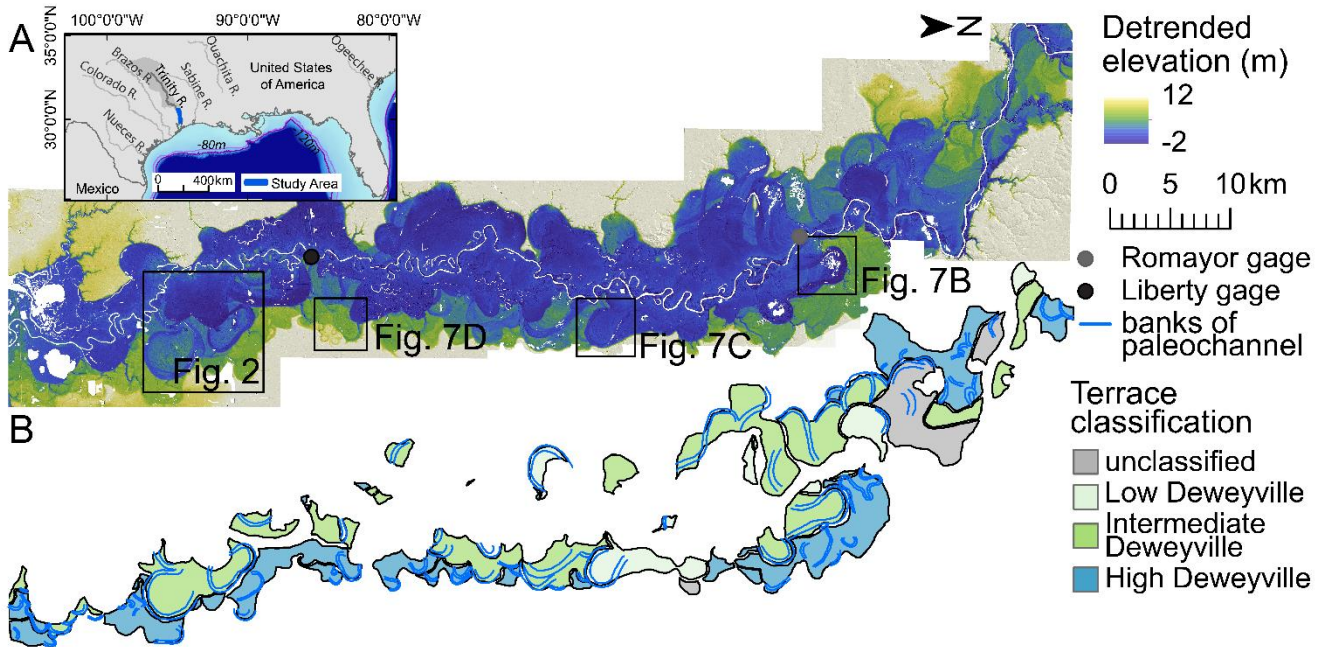
72 It has also been shown that terraces can form by autogenic processes that drive spatially variable incision rates under
73 conditions of persistent, allogenic forced base-level fall (Bull, 1990; Finnegan and Dietrich, 2011; Limaye and Lamb,
74 2014; Merritts et al., 1994; Muto and Steel, 2004; Strong and Paola, 2006). Autogenic terraces can be produced by channel
75 narrowing (Lewin and Macklin, 2003; Muto and Steel, 2004; Strong and Paola, 2006) and river-bend cut off (Erkens et al.,
76 2009), both of which can increase bed incision rates via upstream propagating knickpoints (Finnegan and Dietrich, 2011).
77 Processes that lead to terraces that have autogenic characteristics include local variations in channel dynamics, bedrock slope,
78 and sediment contribution from tributaries (Erkens et al., 2009; Lewin and Macklin, 2003; Womack and Schumm, 1977). In
79 particular, river bend cut-off can locally increase the channel slope, driving channel-bed incision that transitions a segment of
80 floodplain into a terrace (Erkens et al., 2009; Finnegan and Dietrich, 2011). This autogenic trigger produces terrace heights
81 consistent with elevation drops associated with bend cutoffs (Finnegan and Dietrich, 2011). An additional autogenic process
82 that can trigger terrace formation is variable rates of lateral channel migration during persistent base-level fall (Lewin and
83 Macklin, 2003; Limaye and Lamb, 2016). Both unsteady lateral migration and bend cut-off preferentially generate terraces
84 that host only a small number of paleo-channel bends (Finnegan and Dietrich, 2011).

85 Here we present a study of three previously classified sets of fluvial terraces composing the Deweyville Allogroup of
86 the lower Trinity River valley that have previously been described occurring at three distinct elevation trends (Bernard, 1950;
87 Blum et al., 1995; Heinrich et al., 2020; Young et al., 2012). These terraces have been interpreted as forming in response to
88 allogenic triggers that include Pleistocene sea-level fluctuations and climate-controlled changes in water-to-sediment discharge
89 (Anderson et al., 2016; Blum et al., 2013, 1995; Blum and Aslan, 2006; Rodriguez et al., 2005; Saucier and Fleetwood, 1970).
90 We analyze whether these purported allogenic triggers can be distinguished from a null hypothesis that terraces were formed
91 by autogenic processes during long-term valley incision associated with persistent sea-level fall during the Last Glacial Period
92 (from the end of the Eemian to the Last Glacial Maximum). To do this we implement a multi-proxy approach that (1) compares
93 variability in terrace elevations for each classified set against elevation variability for randomly selected terraces, (2) evaluates
94 temporal changes in paleo-hydrology as defined by segments of paleo-channels preserved on terrace surfaces, and (3) relates
95 paleo-slopes defined by the terrace sets to the long profile of the modern Trinity River. Our analysis reveals that the upper set

96 of terraces is most likely the product of an allogenic trigger, while the lowest set of terraces is most likely the product of
97 autogenic processes. The formational driver for the third, intermediate set of terraces is equivocal. This result documents how
98 the study of terraces can be employed to substantially refine paleo-environmental interpretations that are generated using these
99 preserved fragments of relict landscapes.

100 2 Geological Setting

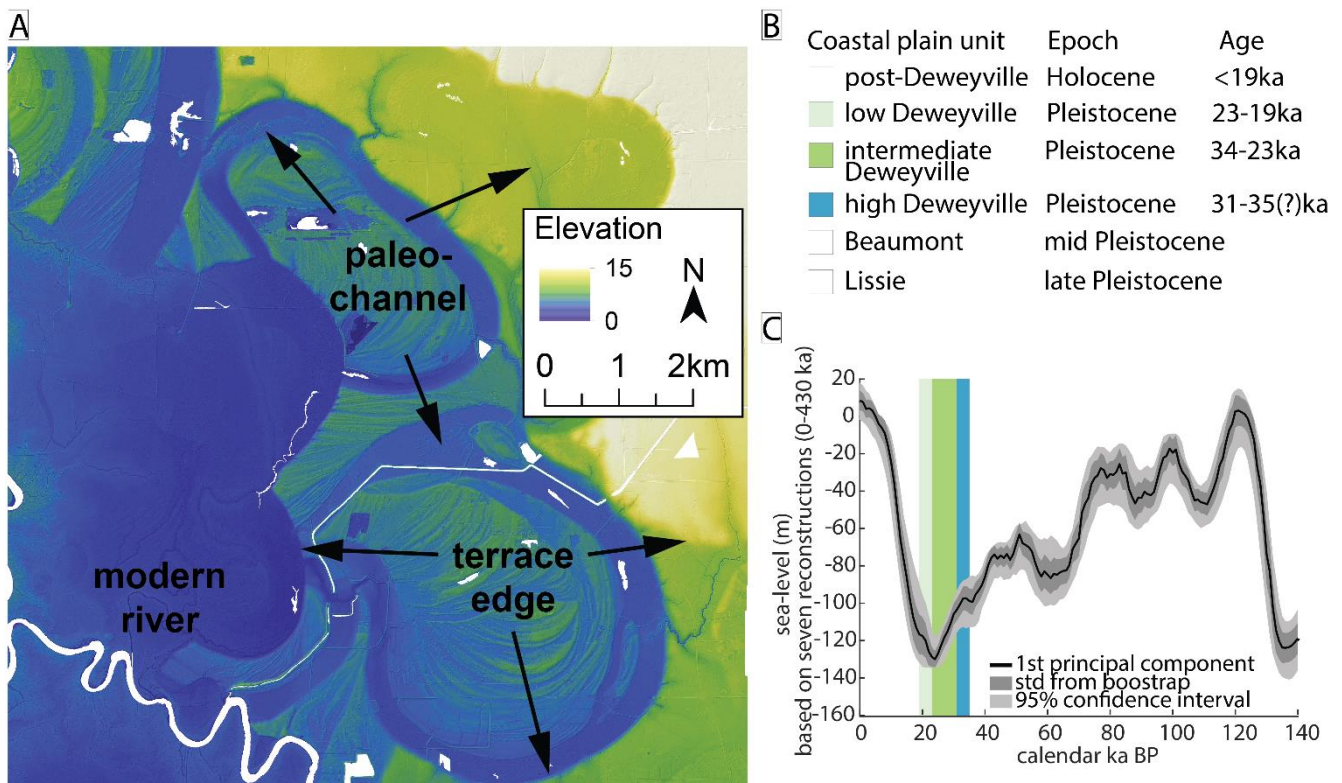
101 The Trinity River has the largest drainage basin contained entirely within the state of Texas, with an area of over
102 46,000 km². It flows from northwest of Dallas, Texas, to Trinity Bay, where it empties into the Gulf of Mexico. Our study area
103 is an ~88 linear-km stretch of the lowermost Trinity River valley from just north of Romayor, Texas, to just north of Wallisville,
104 Texas (**Fig. 1**). Prone to flooding, the Trinity River has a median peak-annual discharge of 1679 m³/s at Romayor, TX (USGS
105 08066500) and 1484 m³/s at Liberty, TX (USGS 08067000) for the 2000 – 2020 hydrograph (U.S. Geological Survey, 2020a,
106 2020b).



107
108 **Figure 1. (A) 2011 bare earth digital elevation model (DEM) from airborne lidar with (B) terrace and paleo-channel outlines of the**
109 **Trinity River, Texas, valley. (A) The lidar DEM has been detrended using the modern valley slope to emphasize local elevation**
110 **variability. The black boxes mark the extent of Fig. 2 and 7B-D. USGS gage stations at Romayor and Liberty are marked in grey**
111 **and black, respectively. The downstream extent of the data is ~10 linear km upstream of the river outlet into the Trinity Bay of the**
112 **Galveston Bay. (B) Terraces are preferentially distributed on the east of the valley.**

113 The Trinity River has been subject to climate and sea-level variations throughout the Quaternary (Anderson et al.,
114 2014; Galloway et al., 2000; Simms et al., 2007); however, the river catchment has never been glaciated and is interpreted to
115 have maintained an approximately constant drainage area over this time (Hidy et al., 2014). The lower Trinity River valley is

116 incised into the Beaumont and Lissie formations of Middle to Late Pleistocene age (Baker, 1995). Within the valley,
 117 Deweyville Allogroup terraces are post-Beaumont in age and formed prior to the Holocene (**Fig. 2A-B**). Age equivalent
 118 terraces with preserved segments of large paleo-channels are also found in alluvial valleys ranging from Mexico to South
 119 Carolina and are often classified as belonging to the same Deweyville Allogroup. Traditionally, the formation of Deweyville
 120 terraces has been interpreted as the product of high frequency Pleistocene sea-level cycles (Anderson et al., 2016; Bernard,
 121 1950; Blum et al., 1995) with distinct episodes of incision and subsequent valley deposition (Blum et al., 2013; Blum and
 122 Aslan, 2006). The history of climatic variation, lack of glaciation, and superb preservation of late Pleistocene terraces make
 123 the lower Trinity River valley an ideal location to study terrace formation and to ask what processes these geomorphic features
 124 record.



125
 126 **Figure 2. (A) Morphological features of the Trinity River valley. Several terraces are preserved at different elevations with the black**
 127 **arrows marking the edges of the terraces. The labelled paleo-channel has a width that is ~2 times the modern river channel width.**
 128 **(B) Regional stratigraphic framework. (C) Global sea-level from seven reconstructions based on (Spratt and Lisiecki, 2016) and**
 129 **Deweyville Allogroup age range (light green, green, and blue).**

130 The Deweyville terraces have been divided into three Allogroups: high, intermediate, and low (Bernard, 1950; Blum
 131 et al., 1995; Young et al., 2012). Sea-level rise during the Holocene has induced valley-floor sedimentation that has partially
 132 buried the low-terrace Allogroup (Blum et al., 1995; Blum and Aslan, 2006). Age control for terraces in the lower Trinity
 133 River valley is limited to eight dates using optically stimulated luminescence (OSL) (Garvin, 2008). Based on these data,

134 Garvin (2008) reports an OSL age of 35 - 31 ka for channel activity on high Deweyville terraces (N = 1), 34 - 23 ka for
135 intermediate Deweyville terraces (N = 4), and 23 - 19 ka for low Deweyville terraces (N = 3). With only a single OSL date
136 from the high Deweyville terraces, these features could be as old as 60-65 ka based on existing stratigraphic frameworks (Blum
137 et al., 2013).

138 The global sea-level curve shows an overall range of ~33m between 35 and 19ka (**Fig. 2C**, Spratt and Lisiecki, 2016).
139 The Pleistocene sea-level curve for the Gulf of Mexico during the period of Deweyville terrace formation shows high-
140 frequency variability superimposed on a longer-term net sea-level fall (Anderson et al., 2016; Simms et al., 2007). Between
141 35 and 19 ka, short-term rises and falls in sea-level are estimated to have been as large as 20 m and 60 m, respectively
142 (Anderson et al., 2016). Deweyville Allogroups have been interpreted to represent three discrete sets of terraces formed during
143 distinct oscillations in sea-level (Anderson et al., 2016; Bernard, 1950; Blum et al., 1995; Morton et al., 1996; Rodriguez et
144 al., 2005; Thomas and Anderson, 1994). The three sets of terraces also have been interpreted as recording episodes of relative
145 sea-level stasis with extensive lateral migration of the river channel, separated by punctuated incision tied to accelerated sea-
146 level fall (Blum et al., 2013; Blum and Aslan, 2006). The commonality between these two interpretations is an allogenic driver
147 for terrace formation.

148 Paleo-channels have long been recognized to record past hydrologic conditions and associated climatic variations
149 (Church, 2006; Knox, 1985). Terraces of the Trinity River valley preserve segments of abandoned river channels that range in
150 apparent widths and depths (**Fig. 2**). Previous researchers have interpreted increases in these paleo-channel widths and radii-
151 of-curvature for paleo-channel bends as products of increases in river discharge and precipitation (Church, 2006; Knox, 1985;
152 Saucier and Fleetwood, 1970; Sylvia and Galloway, 2006), and possible associated changes in vegetation and/or bank
153 erodibility (Alford and Holmes, 1985; Blum et al., 1995; Saucier, 1994). Paleo-channel morphologies thus provide a record of
154 external paleo-environmental change in the lower Trinity River valley that is independent of any signal encapsulated in terrace
155 formation. Therefore, using both terrace elevations and paleo-channels, we have two geomorphic proxies to compare and
156 contrast while assessing terrace formational processes among the Deweyville Allogroups.

157 **3 Null Hypothesis: Terrace Formation**

158 Following the proposal of Limaye and Lamb (2016), our null hypothesis for terrace formation is that punctuated
159 incision by autogenic triggers dominate terrace development. Only after formational mechanisms internal to the system have
160 been considered and rejected, should we consider allogenic triggers for terrace formation. Our method for testing the null
161 hypothesis acts to separate the regional expression of an allogenic driver from more localized terrace production by autogenic
162 processes. It is based on the observation that allogenic triggers produce synchronous, regionally extensive terraces that
163 approximately preserve surface elevations defining a single paleo-valley slope (Bull, 1990; Pazzaglia et al., 1998). It therefore
164 follows that a group of terraces formed by a contemporaneous allogenic trigger should preserve lower variability in elevations
165 about a best-fit plane estimating this paleo-slope than groupings of randomly selected terraces. Conversely, autogenically

166 produced terraces preserve a multitude of elevations that we do not expect to define a contemporaneous long profile. Therefore,
167 groupings of local autogenic terraces are expected to be indistinguishable from sets composed of randomly selected terraces.

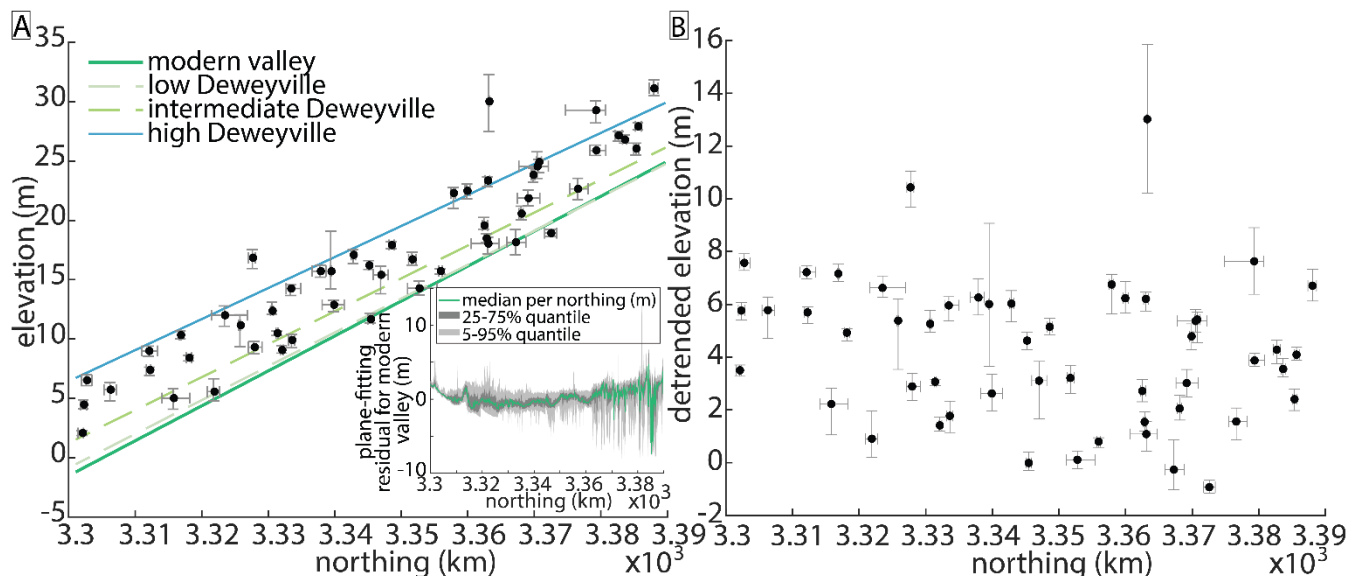
168 **4 Approaches and Observations**

169 Our study used elevation data derived from four airborne lidar surveys collected for the Federal Emergency
170 Management Agency (FEMA) and Texas' Strategic Mapping Program (StartMap) in 2011, 2017, and 2018 (FEMA, 2011;
171 StartMap, 2017a; StartMap, 2017b; StartMap, 2018). These four surveys were merged to produce a single bare earth digital
172 elevation model (DEM) with a 1 m grid spacing. The horizontal accuracies of the four original lidar point clouds from 2011,
173 2017a, 2017b, and 2018 are 0.6 m and 0.4 m, 0.25 m and 0.29 m, 0.20 m and 0.20 m, and 0.20 m and 0.20 m, respectively. All
174 data were referenced to the NAD83 horizontal datum. The vertical accuracy for the original lidar point clouds from 2011,
175 2017a, 2017b, and 2018 are 0.4m, 0.29m, 0.20m, and 0.20m, respectively, and all data were refenced to the NAVD88 vertical
176 datum.

177 Individual terraces and paleo-channels were manually mapped on the merged DEM using ArcGIS. A terrace was
178 defined as a genetically similar surface that is offset in elevation from its surrounding topography. Previously, Blum et al.
179 (1995) mapped terraces on the Trinity River, which was extended by Garvin (2008), using a combination of satellite images
180 and DEMs. Based on these maps, terraces were classified as high, intermediate, or low Deweyville or marked as unclassified
181 if the surface had not been previously identified in Garvin (2008). Care was taken to only map the sections of terrace surfaces
182 that did not appear to be modified by later fluvial processes. Elevations defining each terrace were extracted from the DEM
183 using a 5 m grid resolution for a total of 164,520 measurements across all mapped terraces. A grid resolution lower than the
184 DEM resolution was selected to conserve available computational resources and to speed up analyses. Mapping on the 5-m
185 grid still produced hundreds of points for bare-earth elevation on each terrace, thereby producing estimates for the topography
186 that are comparable to calculations made using the full resolution DEM.

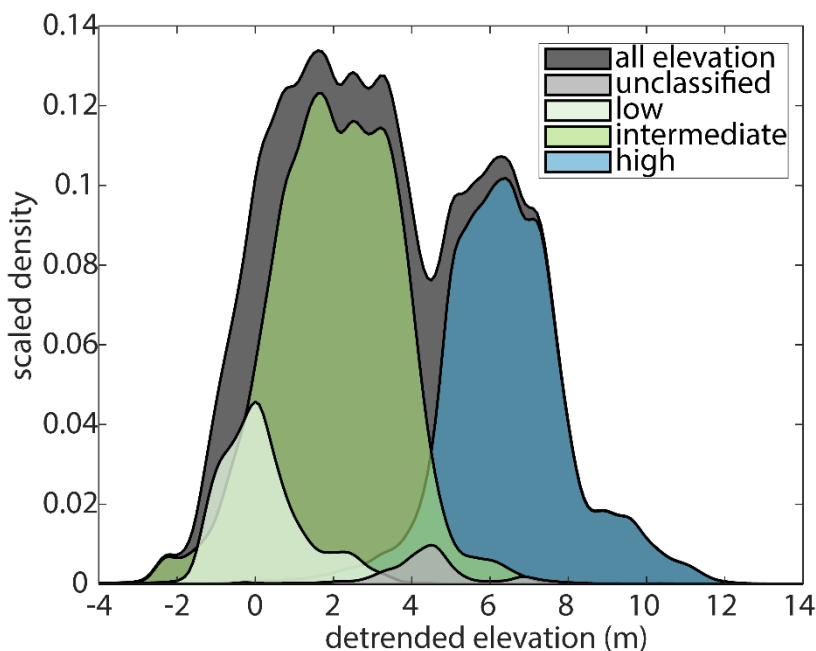
187 From these elevations, the median value and interquartile range were found for each terrace. Since the Trinity River
188 valley in the study area trends N-S, the elevation data for each terrace is plotted against median UTM northing in **Fig. 3A**. A
189 best-fit plane defining the modern valley floor was generated from a subsampled DEM with a 10 m grid resolution. The RMSE
190 of the plane fit is 1.36 m with most of the >4,500,000 points falling within 5m of the plane. Plotting the residuals to the best-
191 fit plane along UTM northing reveals some structure in the most downstream southern long profile extent (**Fig. 3A insert**).
192 However, we do not think this affects our detrended terrace analysis. The plane fit for the modern valley was used to generate
193 detrended elevations for each terrace DEM measurement by subtracting it from the spatially corresponding modern valley
194 best-fit plane value. The detrended median elevations and associated interquartile ranges for each terrace are presented in **Fig.**
195 **3B**. We then compared the distributions of detrended elevations for the terrace classifications. Each classified distribution,
196 scaled to its contribution to the overall number of detrended elevations, is plotted in **Fig. 4**. Even though their median values

197 are different, the detrended elevation distribution for the intermediate Deweyville terraces fully overlaps with that of the low
198 Deweyville terraces (Fig. 4).



199

200 **Figure 3. (A) Median terrace elevation and (B) detrended elevation for the 52 terraces along the N-S trending valley. The error bars**
201 **represent the interquartile range about the median terrace UTM and elevation values. The dark green line corresponds to the**
202 **plane fitted to the 10m DEM of modern valley elevations and the insert shows the residual of this plane fit. Blue, green, and light**
203 **green lines indicate the plane fit to 1m DEM terrace elevations assigned to each terrace category by Blum (1995) and Garvin (2008)**
204 **as high, intermediate, and low Deweyville.**



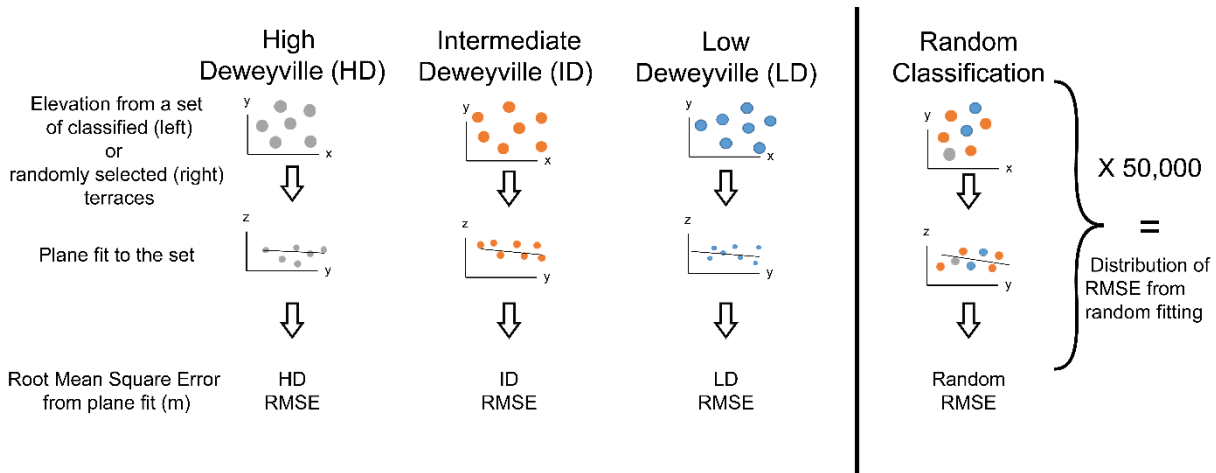
205

206 **Figure 4. Distributions of detrended elevations for terraces classified by Garvin (2008). Distributions were generated using a**
 207 **Gaussian kernel with bandwidth = 0.2 and scaled by the proportion of the total elevation points (164,520) present in each**
 208 **classification. There are 16,543, 84,784, 60,244, and 2960 points in the low, intermediate, high, and unclassified groupings,**
 209 **respectively. There is complete overlap between the detrended elevations of low and intermediate terraces. Terraces classified as**
 210 **high and intermediate have less overlap. The median detrended elevations for the low, intermediate, high, and unclassified**
 211 **Deweyville groupings are 0.3m, 2.05 m, 6.3 m, and 4.41 m.**

212

213 4.1 Testing Terrace Formation using Elevation Data

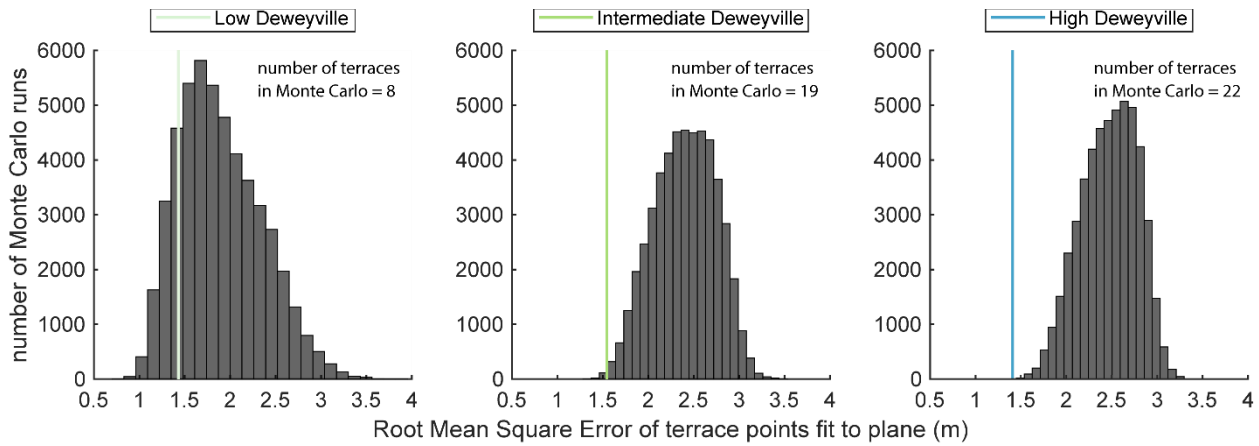
214 We began our hypothesis testing by determining the best-fit plane to all of the elevation points (x, y, z) for terraces
 215 classified into the three Deweyville groups by Blum et al. (1995) and Garvin (2008) using a linear least-squares method. A
 216 planar surface was chosen for this analysis because the modern river-surface and valley profiles are near linear in our area of
 217 study (**Fig. 3A**). The goodness of fit for these three planes to their associated terrace data was captured by the root-mean-
 218 square error (RMSE), which provides a measure of average variability of actual terrace elevations about the best-fit plane (**Fig.**
 219 **5**). The next step was to compare the properties of these fitted planes against planes fit to terraces randomly drawn from the
 220 overall population. The randomly assigned terraces were put into one of three groups that had the same number of elements as
 221 the classified high (n= 22), middle (n=19), and low (n=8) Deweyville terraces. Best-fit planes were calculated and their RMSE
 222 was recorded. This process of randomly assigning terraces into three groups was then repeated 50,000 times in order to derive
 223 a large dataset of elevation variability characterizing randomly grouped terraces (**Fig. 6**).



224

225 **Figure 5. Method to determine if classifications assigned to terraces represent distinct terrace groups. A plane was first fit to**
 226 **elevations extracted from the classified terrace groups in Garvin (2008) at a 5 m grid resolution. We then fit planes to three randomly**
 227 **grouped sets of terraces using the same elevation data, iterating 50,000 times, for a total of 150,000 fits (right of the black line). The**
 228 **root mean square error (RMSE) of the plane fit from each of the previously classified terrace groups was compared to the**
 229 **distribution of RMSE of the randomly grouped terraces (Fig. 6).**

230



231

232 **Figure 6. Root mean square error (RMSE) of a plane fit to elevation points of terraces previously classified as high Deweyville,**
 233 **intermediate Deweyville, and low Deweyville in the Trinity River valley compared to a distribution of RMSE from 150,000 randomly**
 234 **grouped terraces. All of the Deweyville classifications (light green, green, and blue lines) have an RMSE that falls within the**
 235 **distribution of RMSE for randomly grouped terraces. The high Deweyville classification is the closest to falling outside of the**
 236 **distribution, ~3.4 standard deviations away from the random terraces RMSE distribution mean of 2.47 m (22 terrace groupings).**
 237 **The low and intermediate Deweyville classification are ~1.0 and ~2.5 standard deviations away from the RMSE distribution mean**
 238 **of 1.89 m and 2.40 m for 8 and 19 terrace groupings, respectively.**

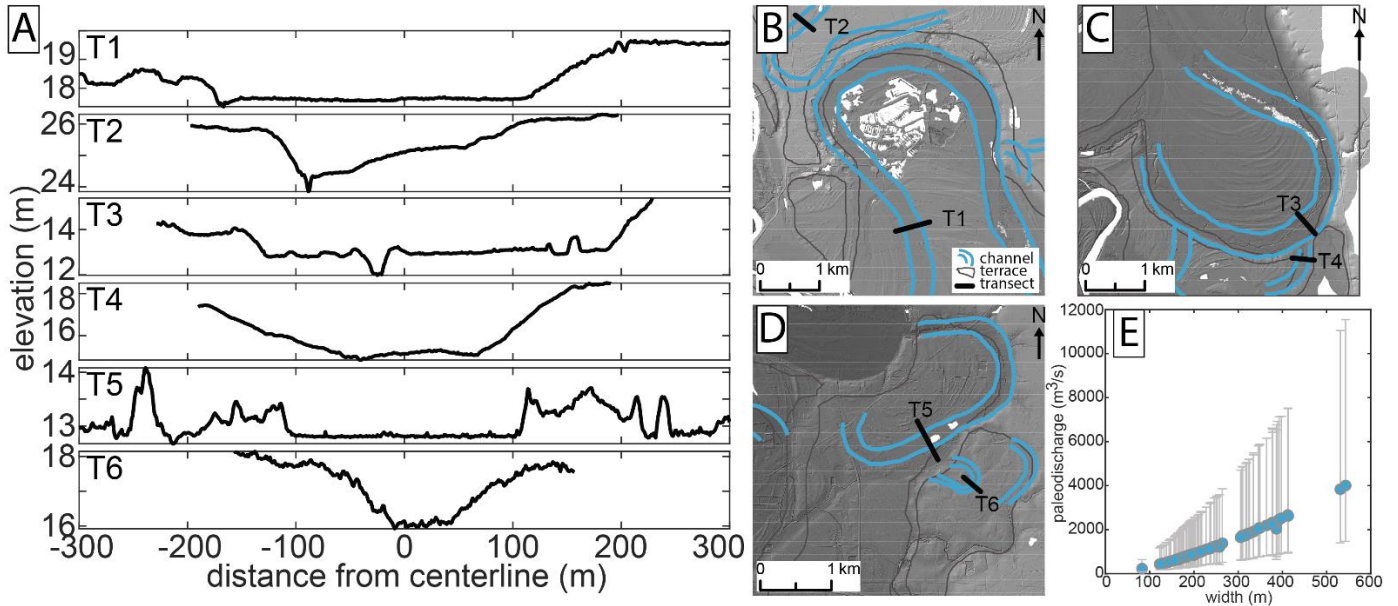
239 4.2 Evaluating Terrace Formation using Paleo-Channel Analysis

240 Change in the discharge of the Trinity River during the late Pleistocene was estimated using the 79 mapped segments
 241 of paleo-channels preserved on terrace surfaces. Mean bankfull width (B_{bf}) for each paleo-channel mapped on the bare-earth
 242 DEM (**Fig. 1B**) was calculated from measurements extracted at 10 m intervals along each paleo-channel centerline (**Fig. 7**).
 243 Representative sidewall slopes (rise/run) for these paleo-channels range between 0.02 and 0.26 (**Fig. 7A**). These paleo-sidewall
 244 slopes fall within the range of modern sidewall slopes measured for the Trinity River in the study area by Smith and Mohrig,
 245 (2017, their Fig. 4). Therefore, we confidently use the paleo-channel widths extracted from the DEM without any correction
 246 to the widths associated with relaxation of the paleo-topography over time. These data were used to estimate a formative,
 247 bankfull discharge (Q_{bf}) for sand-bed rivers following the hydraulic geometry relationship developed by Wilkerson and Parker,
 248 (2011):

$$249 \frac{B_{bf} * g^{\frac{1}{5}}}{Q_{bf}^{\frac{2}{5}}} = 0.0398 * \left(\frac{D_{50} * \sqrt{R * g * D_{50}}}{\nu} \right)^{0.494 \pm 0.14} * \left(\frac{Q_{bf}}{D_{50}^2 * \sqrt{g * D_{50}}} \right)^{0.269 \pm 0.031}, \quad (1)$$

250 where ν is the kinematic viscosity of water, R is the specific gravity of the sediment ($R = \frac{\rho_s - \rho}{\rho}$), ρ_s is sediment density, ρ is
 251 water density, g is gravitational acceleration, and D_{50} is the median grain size of transported bed material. We used a value of
 252 2650 kg/m^3 for ρ_s and a range of paleo-channel grain sizes taken from Garvin (2008), who sampled both the lower and upper
 253 portions of bar deposits within preserved channel fills (**Table 1**). The uncertainty in estimated discharge was quantified for
 254 each paleo-channel using Monte Carlo simulation. For each run of the simulation, we sampled from: (1) normal distributions
 255 with the reported means and standard deviations for each exponent in **Eq. 1**; (2) a normal distribution for channel width using

256 its measured mean and standard deviation; and (3) a uniform distribution of grain sizes constrained by measurements from
 257 each classified terrace set (**Table 1**). This Monte Carlo simulation was run 50,000 times for each paleo-channel. Paleo-
 258 discharge estimates derived for the 79 channel segments preserved on terrace surfaces are plotted as a function of median
 259 detrended terrace elevation in **Fig. 8**.

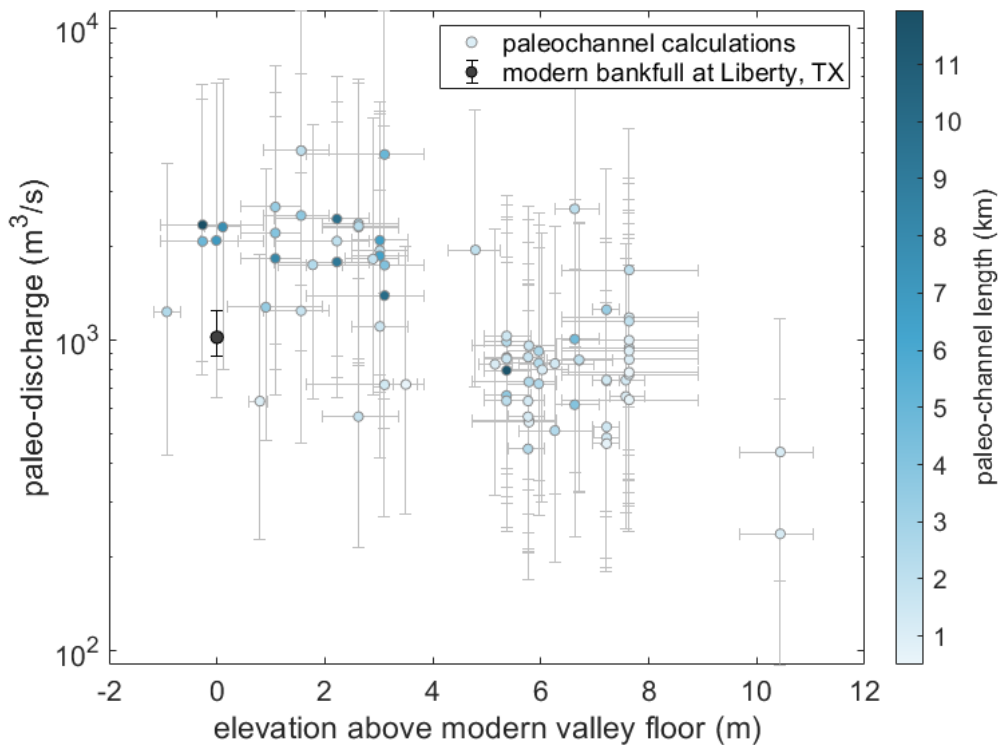


260

261 **Figure 7: Paleo-channel widths and paleo-discharge estimates.** (A) Elevation transects for six paleo-channels (T1-T6). Transects are
 262 taken from locations indicated in (B)-(D) with mapped paleo-channels outlined in blue and terrace extents mapped outlined in grey.
 263 (E) Paleo-discharge estimates for the Trinity River are plotted as a function of their width. Each paleo-discharge was calculate using
 264 preserved channel width measurements and the discharge-width relationship from Wilkerson and Parker (2011) (Eq. 1). Error bars
 265 represent the first and third quartile of paleo-channel discharge estimates.

Garvin (2008) Terrace classification	Upper bar deposit lower range (mm)	Upper bar deposit upper range (mm)	Lower bar deposit lower range (mm)	Lower bar deposit upper range (mm)	Average grain size (mm)
Low Deweyville	0.25	1.00	0.25	4.00	0.71
Middle Deweyville	0.125	1.00	0.50	2.00	0.59
High Deweyville	0.125	2.00	0.25	2.00	0.59

266 **Table 1: Grain size of terrace deposits from Garvin (2008), used for discharge calculations. The average grain size was calculated**
 267 **using the phi (logarithmic) scale.**



268

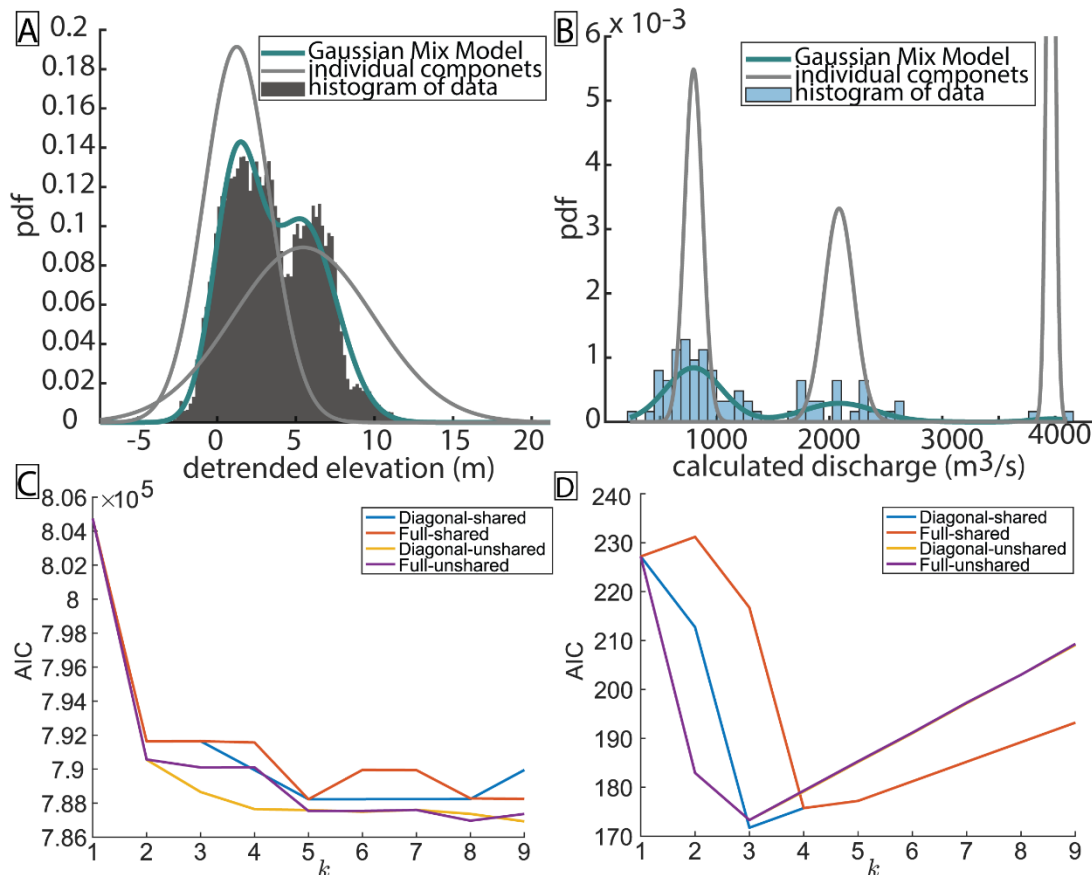
269 **Figure 8. Paleo-discharge estimates for the Trinity River plotted as a function of their associated detrended terrace elevations.**
 270 **Detrended elevations afford a crude stratigraphy for the discharges with the highest relative elevations representing older channels**
 271 **and lowest elevations representing younger channels. Each paleo-discharge was calculated using preserved channel width**
 272 **measurements and the discharge-width relationship from Wilkerson and Parker (2011) (Eq. 1). Error bars represent the first and**
 273 **third quartile of paleo-channel discharge estimates and terrace elevations above the modern valley. The symbol was shaded to the**
 274 **preserved length for each paleo-channel, with darker symbols equated to longer segments. The modern bankfull discharge at**
 275 **Liberty, TX was found using the methods described in the text, and plotted at 0m.**

276 Accuracy of the Wilkerson and Parker (2011) relationship for the Trinity River system was tested by calculating a Q_{bf} value
 277 for the modern river channel and comparing it against the bankfull discharge logged at the USGS gage 08067000 at Liberty,
 278 Texas. The calculated bankfull discharge was estimated using the measured bankfull width of 170 m from the DEM at the
 279 gage site. The median particle size of bed material at Liberty has been measured at 200 μ m by the Trinity River Authority of
 280 Texas (Trinity River Authority of Texas, 2017). All other variables in **Eq. 1** were kept constant between the modern river and
 281 paleo-channels, yielding an estimate for the modern bankfull discharge of 830 m³/s. The reported residual standard error
 282 associated with the bankfull discharge **Eq. 1** (Wilkerson and Parker, 2011) was then used to approximate the error associated
 283 with this modern calculated bankfull discharge. The lower and upper standard error define a possible range between 340 and
 284 2030 m³/s. These discharges estimated with **Eq. 1** compare favorably with the measured discharge found using the rating curve
 285 for the USGS Liberty gage station (https://waterdata.usgs.gov/nwisweb/get_ratings?file_type=exsa&site_no=08067000) and
 286 bank-line elevations for the swath of channel extending 300 m both upstream and downstream of the gage. The mean and

287 standard deviation of bank elevations for this swath was 7.68m and 0.34m, yielding a mean bankfull discharge of 1017 m³/s
 288 and discharges of 887 m³/s and 1243 m³/s corresponding to stages ± 1 standard deviation in bank elevation.

289 4.3 Mixing Models and Bend Cutoff Analyses

290 To test the existence of statistical groupings within our terrace and paleo-channel data, a mixing model was used to generate
 291 Gaussian mixture distributions that were fitted to both the 164,520 detrended terrace elevation points and the median discharges
 292 estimated for the 79 paleo-channel segments (**Fig. 9**). Results are used to determine if Deweyville terraces should be divided
 293 into three distinct sets. The Akaike Information Criterion (AIC) and Bayesian Information Criterion (BIC) were applied to
 294 both mixing models in order to optimize the number of components used to represent each distribution (**Fig. 9C, 9D**). Two
 295 and three components were selected for the distributions of detrended elevation points and median paleo-channel discharges,
 296 respectively (**Fig. 9A, 9B**).



297
 298 **Figure 9. Mixing model fits to measured distributions of terrace elevation and estimated paleo-discharges. Distributions using (A)**
 299 **elevation and (B) paleo-channels support an interpretation of allogenic forcing for high terrace abandonment due to increasing**
 300 **discharge. Akaike Information Criterion (AIC) for (C) detrended elevation and (D) paleo-discharge mixing model. BIC results are**
 301 **not shown here but have similar trends to AIC. AIC results are shown for the mixing model that are solved for a diagonal and full**

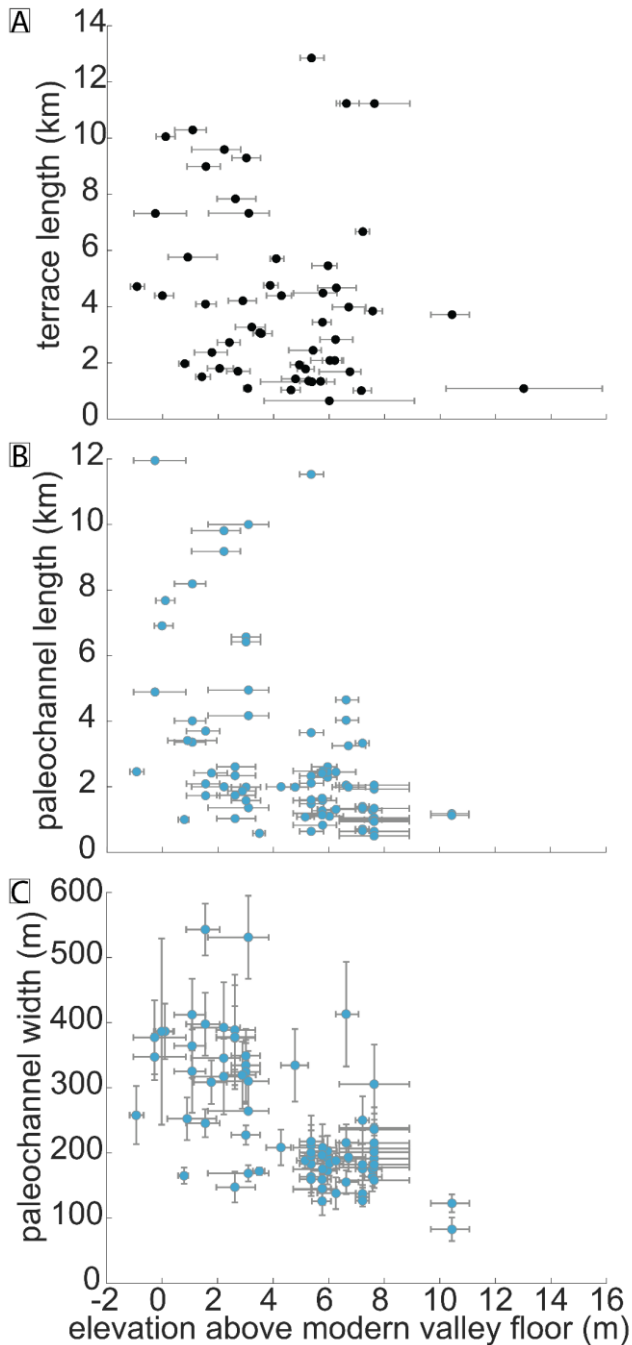
302 covariance matrix and shared and unshared covariance. The model also used a small Regularization value to ensure the estimated
303 covariance matrix is positive.

304 An important additional measurement used to assess whether terraces were abandoned due to enhanced local incision
305 driven by gradient change during channel bend cut-off was the elevation differences between 40 adjacent terraces. These
306 connections can first be assessed by comparing the minimum bounding box length of terraces, paleo-channel width, and paleo-
307 channel length (**Fig. 10**). These measured elevation differences between terraces were compared to estimated elevation changes
308 produced by bend cut-offs. We used **Eq. 2** to calculate the elevation drop produced by a bend cutoff as:

$$\Delta elevation_{bend\ cutoff} = length_{bend} * slope_{channel} \quad (2)$$

309 On several low, intermediate, and high Deweyville terraces, the lengths of paleo-channels that had one bend preserved were
310 measured using the bare-earth DEM (e.g., **Fig. 2**). The mean and standard deviations for bend lengths on the low, intermediate
311 and high terraces are 5.7 ± 2.8 km (n = 3), 4.6 ± 3.0 km (n = 10), and 2.3 ± 1.1 km (n = 11), respectively. The overall distribution
312 above the modern valley floor of paleochannel lengths plotted in **Figure 10B**. We approximated channel slope using the planes
313 fit to the terrace elevation points for each classification. The calculated mean slope and standard error for the low, intermediate,
314 and high terraces are 3.0×10^{-4} (3.1×10^{-6}), 2.9×10^{-4} (1.10×10^{-6}), and 3.0×10^{-4} (1.2×10^{-6}), respectively. Using Equation 2,

315 estimated elevation drops driven by a possible bend cut-off are 1.6 ± 0.8 m, 1.3 ± 0.9 m, and 0.7 ± 0.3 m (**Fig. 11A**).



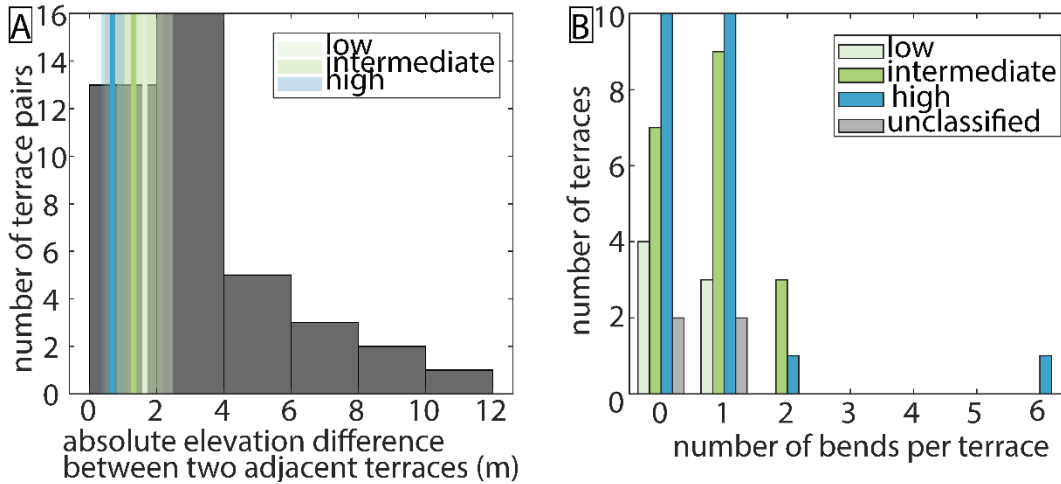
316

317 **Figure 10 (A) terrace length, (B) paleo-channel length, and (C) paleo-channel width plotted along the median elevation of the**

318 **associated terrace above the modern valley floor plane. The youngest terraces are more likely to have larger terrace lengths as well**

319 as paleochannel lengths. Terrace length was measured as the longest length of a minimum bounding box envelop for each terrace.
 320 These envelopes were defined with edges in the N-S and E-W direction. Error bars show the interquartile range of each terrace.

321 An additional measurement used to evaluate the likelihood of terraces being produced by bend cut-off was the largest
 322 number of channel bends present in a segment of paleo-channel preserved on a terrace surface. The number of channel bends
 323 preserved on terrace surfaces can be used as an indicator for autogenic versus allogenic processes, whereby allogenic terrace
 324 formation likely abandons larger paleo-floodplain sections, preserving multiple channel bends. For incising rivers, the
 325 autogenic cut off of a single meander bend has been shown to be sufficient to produce the enhanced channel erosion required
 326 to elevate relatively small sections of the previous active floodplain above flood levels (Finnegan and Dietrich, 2011).



327
 328 **Figure 11. Terrace properties used to assess the likelihood of meander bend-cutoff being the driver of terrace formation. (A)**
 329 **Differences in elevation between adjacent terrace surfaces. Also plotted as vertical lines and swaths are the mean values \pm 1 standard**
 330 **deviation for elevation decreases expected from cutting off a single meander bend for paleo-channels of the low, intermediate, and**
 331 **high Deweyville Allogroups. (B) Maximum number of paleo-meander bends preserved in a channel segment on each terrace. Most**
 332 **terraces have between 0-1 channel bends preserved for one generation of channel. Only intermediate and high Deweyville terraces**
 333 **have more than two channel bends preserved by a paleo-channel.**

334 4. Summary of observations

335 We mapped 52 terraces and 79 paleo-channel segments in the study area (**Fig. 1B**). Of these terraces, 22 are classified
 336 as high Deweyville, 19 as intermediate Deweyville, 8 as low Deweyville, and 4 were left unclassified as they could not be
 337 correlated with terraces mapped by either Blum et al. (1995) or Garvin (2008). The low, intermediate, and high Deweyville
 338 terraces have median values for detrended elevations of 0.03 m, 2.06 m, and 6.37 m. Based on our mixture modeling, the mean
 339 and standard deviation of the detrended elevation components are 5.6 ± 4.18 m and 1.32 ± 2.19 m with mixing proportions of
 340 0.51 and 0.49, respectively. Similarly, the mean and standard deviation for the three Gaussian distributions describing paleo-
 341 discharges are 795 ± 80 m³/s, 2083 ± 139 m³/s, and 4013 ± 21 m³/s with mixing proportions of 0.68, 0.30, and 0.02,
 342 respectively. Terraces vary in both size and shape, although they are typically elongate parallel to the valley axis and continuous
 343 for less than 10 km in that direction. The distribution of terraces is asymmetric, with more terraces observed on the east side

344 of the valley (**Fig. 1B**). Consequently, most terraces are unpaired, meaning they have no topographic equivalent on the opposite
345 side of the valley.

346 The best-fit planes to elevations for the Deweyville terrace groups defined by Blum et al. (1995), Garvin (2008), and
347 Hidy et al. (2014) show remarkably similar slopes amongst terrace sets. The slopes and standard error for the low, intermediate,
348 and high terraces are 3.0×10^{-4} (3.1×10^{-6}), 2.9×10^{-4} (1.10×10^{-6}), and 3.0×10^{-4} (1.2×10^{-6}), respectively. These paleo-slopes are
349 indistinguishable from the estimated slope for the modern valley of 3.0×10^{-4} (8.0×10^{-8}) (**Fig. 3A**). It is not surprising that all
350 four profiles are well fit by planes given the fact that the studied river segment represents less than ten percent of the modern
351 river length and both grain size and discharge vary little over the studied reach.

352 Plane fits for the low, intermediate, and high Deweyville terrace sets have RMSEs of 1.43m, 1.54m, and 1.41m,
353 respectively. Values of RMSE for best-fit planes to randomly grouped terraces are sensitive to the number of terraces defining
354 a group. The fewer the number of terraces, the more likely it is that a low RMSE will result (**Fig. 6**). It is therefore important
355 when comparing randomly grouped terraces to the previously classified groups that the number of terraces in each be the same.
356 Running our analysis of 50,000 sets of randomly assembled terraces with the same number of elements as the low ($n=8$),
357 intermediate ($n=19$) and high ($n=22$) Deweyville groups yielded the following RMSE results. The median and interquartile
358 values of RMSE for planes fit to randomly selected terraces of the number present in the low-terrace classification are 1.82m,
359 1.55m, and 2.21m. The median and interquartile values of RMSE for planes fit to randomly selected terraces of the number
360 present in the intermediate-terrace classification are 2.41m, 2.15m, and 2.66m. And finally, the median and interquartile values
361 of RMSE for planes fit to randomly selected terraces of the number present in the high-terrace classification are 2.49m, 2.25m,
362 and 2.71m.

363 The RMSE values for the best-fit planes to the classified Deweyville terraces are plotted on their associated synthetic
364 RMSE distributions for randomly selected terraces in **Fig. 6**. Inspection of **Fig. 6** reveals little overlap between the classified
365 high terraces and the random samplings of terraces. For the high Deweyville case, there was only a 0.008% occurrence of
366 randomly selected terraces yielding an RMSE as low as 1.41m. A very different result was found for the classified low terraces,
367 where its RMSE falls well within the associated distribution of synthetic RMSEs with fully 21% of all randomly selected cases
368 having lower RMSE values. Minimal overlap was found between the RMSE for the classified intermediate terraces and the
369 distribution of RMSE values generated from random terrace groupings. Only 1% of the randomly selected sets terraces were
370 better fit to a plane than the classified group of intermediate terraces. Mapped paleo-channels have widths that range from 82
371 to 543 m (**Fig. 7**). Estimated bankfull discharges calculated using these widths (**Eq. 1**) range from $233 \text{ m}^3/\text{s}$ to more than 4000
372 m^3/s (**Fig. 8**). These paleo-discharges cluster into two groups, one at lower discharges centered around $795 \pm 80 \text{ m}^3/\text{s}$ and one
373 at higher discharges centered on $2083 \pm 139 \text{ m}^3/\text{s}$ (**Fig. 9B**). The grouping of lower-discharge paleo-channels sit on terraces
374 that have median elevations $>4.5 \text{ m}$ above the modern valley floor and correspond to high Deweyville terraces (**Fig. 8**). The
375 grouping of higher-discharge paleo-channels is preserved on terraces that have median elevations from 0.2 m below to 5.2 m
376 above the modern floodplain and correspond to both intermediate and low Deweyville terraces (**Fig. 8**). The investigation of
377 paleo-channel characteristics revealed that paleo-channel widths, paleo-channel lengths, and overall terrace lengths all are

378 more likely to be greater for younger terraces (**Fig. 10**). Most terraces have one or fewer channel bends preserved (**Fig. 11B**)
379 and only the intermediate and high Deweyville classifications possess terraces with more than two preserved channel bends.

380 **5 Discussion and Conclusions**

381 Late Pleistocene terraces of the lower Trinity River valley formed during a period of net sea-level fall punctuated by
382 shorter and smaller magnitude fluctuations (Anderson et al., 2016). Previous researchers have interpreted the formation of the
383 Trinity terraces, as well as those observed in other Texas coastal valleys, in the context of these fluctuations (Blum et al., 1995;
384 Blum and Aslan, 2006; Morton et al., 1996; Rodriguez et al., 2005). However, it has also been suggested that this terrace
385 formation in the lower Trinity River valley was driven by autogenic triggers (Guerit et al., 2020). The motivation for this study
386 was to develop tools to help distinguish between these two forcings that can produce terraces.

387 Several morphological characteristics exist to describe both the Trinity River terraces and their associated paleo-
388 channels. The terraces are most commonly unpaired (**Fig. 1**), which is expected during autogenic terrace formation associated
389 with unsteady lateral migration rates during formation (Bull, 1990; Merritts et al., 1994) and river bend cut-off (Finnegan and
390 Dietrich, 2011). On the flip side, paired terraces can also be formed during constant, albeit low vertical incision rates, during
391 lateral migration (Limaye and Lamb, 2016). Unpaired terraces can also be produced by unequal lateral river erosion post
392 terrace formation that preferentially removes half of a previously formed pair of allogenic terraces (Malatesta et al., 2017).
393 Similarly, lateral migration also affects the age distribution of the terraces preserved because younger terraces, closer to the
394 modern river are more likely to eroded away than older terraces (Lewin and Macklin, 2003; Limaye and Lamb, 2016). The
395 presence of unpaired terraces in the lower Trinity River valley may therefore be most indicative of the relative importance of
396 lateral migration for this system.

397 For the Trinity River, many of the valley-ward edges of the lower and intermediate Deweyville Allogroups have the
398 shapes of meander bends, recording the most outward extent of the active channel before the floodplain surface was abandoned
399 (**Fig. 1, Fig. 2**). We take this as evidence for the autogenic process of channel cutoff triggering terrace formation. The observed
400 elevation differences between adjacent terraces are also consistent with those predicted by cut off of a single meander bend
401 (**Fig. 11A**). Similar interpretations have also been made for strath terraces in bedrock (Finnegan and Dietrich, 2011).
402 Furthermore, their tendency to be preserved as unpaired terraces with a small number (< 2) of channel bends is more consistent
403 with the stochastic nature of meander cutoffs by autogenic processes than large-scale incisional events due to allogenic forcings
404 (**Fig. 11A & 11B**, Finnegan and Dietrich, 2011). Therefore, the morphology of the Trinity River valley terraces alone is
405 suggestive of an autogenic forcing, but likely not sufficient to distinguish between allogenic versus autogenic terrace formation.

406 We argue that a robust test for assessing the likelihood of autogenic versus allogenic forcing in terrace formation
407 comes from an analysis of the topographic variability of terrace sets inferred to have formed synchronously. Here we have
408 developed a method to quantitatively compare elevation variability of any classified group of terraces against randomly
409 selected terrace sets (**Fig. 5, Fig. 6**) so that we can evaluate whether a classified group is better organized than arbitrarily
410 selected ones. For the lower Trinity River valley, if the Deweyville terraces formed synchronously (Blum et al., 1995; Blum

411 and Aslan, 2006; Morton et al., 1996; Rodriguez et al., 2005), one would predict that terraces within these groups would show
412 lower variation about a best-fit plane than randomly grouped terraces (**Fig. 6**). Limaye and Lamb (2016) defined a unique
413 elevation set as surfaces that are separated by more than 1m. They found that lateral migration during a constant incision rate
414 versus pulsed incision rates can result in similar and indistinguishable terrace sets (Limaye and Lamb, 2016). Our approach
415 builds on this idea and develops a framework that evaluates the magnitudes of variations in elevation amongst terraces
416 compared to a fitted plane for the set. This approach is especially useful for studies where age control across terraces is not
417 well constrained. Since we are assessing many elevation points from each terrace in the terrace set, it is possible to tease apart
418 long profile variations for terrace sets only vertically separated by ~1m.

419 Our RMSE results show that the best-fit plane for the low Deweyville Allogroup cannot be separated from, and is
420 instead consistent with, sets of randomly grouped terraces mimicking autogenic processes of either bend cutoff or of unsteady
421 river lateral migration during constant base level fall (**Fig. 6B**). The driver for the intermediate Deweyville Allogroup cannot
422 be unambiguously determined based on the RMSE analysis. The classified group is better organized than most, but not all,
423 randomly generated groupings of terraces (**Fig. 6C**). The overlap leads us to presume that the null hypothesis of autogenic
424 terrace formation cannot be robustly falsified. A different conclusion was reached for the high Deweyville Allogroup. With
425 our RMSE analysis, we reject the null hypothesis of autogenic terrace formation. The high Deweyville Allogroup is most likely
426 the product of punctuated allogenic change with an RMSE that is as small as any of the 50,000 values generated for random
427 groupings of terraces (**Fig. 6A**). A difference between the low/intermediate versus high terraces was also found in the
428 distribution of detrended terrace elevations using a 2 component Gaussian mixing model. The first component of this model
429 overlaps with elevations classified as low and intermediate Deweyville, while the second component corresponds most closely
430 to high Deweyville elevations (**Fig. 4, Fig. 9A**). We, therefore, conclude that the high Deweyville terraces are different than
431 the other two sets and record an allogenic signal connected with early valley incision. This new analysis likely means that
432 across a relatively short interval of time, <10 kyr, terraces on the Trinity River switched from recording an allogenic trigger in
433 the high Deweyville Allogroup to being indistinguishable from terraces formed by autogenic triggers such as bend cut-off or
434 unsteady lateral migration rates.

435 The connections between potential discharge changes and terrace formation were assessed using paleo-channel widths
436 and grain size (**Fig. 8, Fig. 9B**). Paleo-channel discharge estimates reveal a factor of two increase in bankfull discharge moving
437 from older, high Deweyville terraces to younger, intermediate, and low Deweyville terraces. The estimated changes through
438 time in bankfull discharge are not matched by estimated changes in river long-profile or paleo-slope. Previously discussed
439 best-fit planes to the Deweyville Allogroups have slopes that are roughly constant and indistinguishable from the modern long
440 profile for the Trinity River (**Fig. 3A**). Theory by Parker et al. (1998) and experiments by Whipple et al., (1998) have
441 demonstrated long-profile slope for sandy fluvial systems is a function of sediment-to-water discharges. Terraces associated
442 with base-level fall have been shown to maintain consistent valley slopes (Tofelde et al., 2019). Experiments by the same
443 authors also showed that sediment and/or water discharge changes produce changing slopes for terrace sets, which we do not
444 observe here. We suspect that the switch in discharge is not directly recorded in the terrace elevation because the change in

445 water discharge appears to have been approximately matched by a sediment-flux increase, as recorded in the constant long-
446 profile slope for the paleo-river. With no slope reduction, no incision would have occurred. As a result, discharge changes
447 recorded by segments of paleo-channels on the intermediate and low Deweyville terraces are not interpreted to have driven
448 incision and terrace formation. Instead, it is likely that an autogenic trigger associated with persistent base-level fall drove the
449 terracing. Recent synthesis studies by Phillips and Jerolmack (2016) and Dunne and Jerolmack (2018) confirm that these
450 estimates of bankfull discharge are tied to moderate flooding and representative of mean climate properties. While our
451 estimated discharge changes over the latest Pleistocene are large, it is only half of the proposed four times increase reported
452 for similar paleo-channels preserved on terraces of the nearby lower Brazos River valley (Sylvia and Galloway, 2006).

453 Maintenance of a roughly constant slope while water discharge changed therefore almost certainly required
454 commensurate changes to sediment discharge. We can test this change in sediment discharge by looking at results from existing
455 studies. An increase in sediment discharge is in agreement with Anderson (2005), who suggests that sediment discharge was
456 greater during the LGM than today. However, calculations for the Trinity River by other authors do not currently reflect these
457 changes. Sediment discharges have been estimated to decrease during the LGM (intermediate and low Deweyville) based on
458 the BAQRT model by Syvitski and Milliman (2007) (Blum and Hattier-Womack, 2009; Garvin, 2008). Hidy et al. (2014) also
459 calculated ^{10}Be denudation rates and suggested that upstream weathering was greater during the interglacial periods and that
460 reworking of stored sediments was greater during glacial periods. However, Hidy et al. (2014) was not able to combine the
461 effects of reworking and upstream sediment flux using ^{10}Be to estimate the sediment discharge associated with terrace
462 formation. More recent methods were developed to estimate sediment discharge based on bedforms and stratigraphy, which
463 are exposed along the Trinity River (Mahon and McElroy, 2018). Therefore, there is also an opportunity to refine and improve
464 sediment discharge estimates for Deweyville terraces. Regardless, responsive adjustments to sediment discharge suggest that
465 throughout the latest Pleistocene, the river itself remained a predominantly transport limited system (Howard, 1980; Whipple,
466 2002).

467 Understanding the cut off of a river bend is important to identify autogenic triggers for terrace formation. We have
468 shown that a majority of Deweyville terraces in the Trinity valley preserve no more than a single paleo-channel bend (**Fig.**
469 **11B**) and that elevation differences between adjacent terraces are similar to an expected elevation change driven by channel
470 shortening through cut off to a river bend (**Fig. 11A**). These terrace properties highlight an opportunity for our community to
471 measure the number of bends involved in the autogenic shortening of river channels. Specifically, there is an opportunity to
472 quantify what percentage of cutoffs result in two or more bends being detached from the active channel in short amounts of
473 time, thereby refining an expected upper limit to the number of channel bends preserved on autogenically generated terraces.
474 Exceptionally preserved paleo-channels such as on the Trinity River, provide this opportunity to distinguish autogenic
475 processes responsible for terrace formation, and as such might provide a more faithful record of changes in discharge to the
476 system than terrace elevations and morphologies. An additional mechanism for reducing uncertainty in the processes that cut
477 Trinity terraces would be assembling a greater number of terrace ages. Increasing age control could constrain vertical versus

478 lateral migration rates for the river to a point where autogenic versus allogenic processes connected to terrace formation are
479 separable (Limaye and Lamb, 2016; Merritts et al., 1994).

480 Irrespective of terraces formation, other river systems across the southeastern United States have the potential to also
481 record a step-increase in formative discharge seen in the Trinity valley between the high to intermediate/low Deweyville
482 terraces. This change was likely driven by a wetter climate in southeast Texas during the period ~34–20 ka, based on OSL
483 dates for the low and intermediate Deweyville terraces (Garvin, 2008). During the Last Glacial Maximum (19-26 ka),
484 precipitation in western and southwestern USA has been shown to be ~0.75–1.5 and ~1.3-1.6 of modern, respectively (Ibarra
485 et al., 2018). Additionally, GCM models show a general increase in precipitation in the study area during the late Pleistocene
486 (Roberts et al., 2014 (Fig. 2); McGee et al., 2018 (Fig. 2)). Our observations agree with other workers who interpreted the
487 changes in channel size as an increase in mean discharge during this period (Alford and Holmes, 1985; Gagliano and Thom,
488 1967; Saucier and Fleetwood, 1970; Sylvia and Galloway, 2006). Observations of larger paleo-channels during this period are
489 also seen across rivers in the southeast of Texas (e.g. Bernard, 1950; Blum et al., 1995; Sylvia and Galloway, 2006), Arkansas
490 and Louisiana (e.g. Saucier and Fleetwood, 1970), and Georgia and South Carolina (e.g. Leigh and Feeney, 1995; Leigh et al.,
491 2004; Leigh, 2008).

492 Our contribution to the existing work on terraces in this region is to reconcile the literature that suggests an episodic
493 cut and fill and/or base level change model (Blum et al., 1995) with the literature on terrace formation due to increased
494 discharge (Sylvia and Galloway, 2006). While both have the potential to generate terraces, intrinsic processes such as bend
495 cut-off and unsteady lateral migration during constant base level fall need to first be ruled out. For example, relatively slow
496 vertical incision rates especially, pulsed discharge changes (allogenic process) and unsteady lateral migration (autogenic
497 process) showed indistinguishable morphologies in Limaye and Lamb (2016). Here, for all but the high Deweyville, autogenic
498 triggers for terrace development cannot be ruled out.

499 The results presented here demonstrate that it is critical to understand the many potential forcings (both allogenic and
500 autogenic) on a river system that can lead to terrace formation and to employ robust, quantitative tests for discriminating
501 between these forcings before using terraces to reconstruct paleo-environmental histories. The method proposed here for
502 assessing the role of allogenic processes in terrace formation using the variability of terrace elevations provides a simple,
503 quantitative test, and may prove useful for interpreting terrace formation in other river systems. We were not able to correlate
504 terrace levels back to distinct trigger events, although allogenic forcings such as sea-level fluctuations and discharge changes
505 were also classified here. We suggest that paleo-channel characteristics are a more faithful record of discharge changes in
506 fluvial systems and that additional bend metrics introduce can differentiate autogenic terrace formation processes, specifically
507 bend cut-off from unsteady lateral migration rates.

508 **Data availability**

509 The lidar dataset was acquired from the Texas Natural Resource Information System (TNRIS) at <https://tnris.org>. Please see
510 the reference to each dataset. Tables with analysis produced from the lidar datasets are included in the supplementary material.

511 **Author contribution**

512 All authors designed the analysis and contributed to the manuscript writing. HHG and TE analyzed the lidar dataset. TG
513 developed the code to fit planes to the lidar dataset.

514 **Competing interests**

515 The authors declare that they have no conflict of interest.

516 **Acknowledgments**

517 We thank Webster Mangham for providing the report from the Trinity River Authority of Texas Phase II, Bathymetry and
518 Sediment Collection for the Port of Liberty Study. We thank Ajay Limaye and one anonymous reviewer and Ajay Limaye for
519 constructive reviews. We also thank Joel Johnson and Gary Kocurek for insightful comments on early versions of the
520 manuscript as well as Niels Hovius, Mike Lamb, Paola Passalacqua, and Daniella Rempe for additional comments. HHG was
521 funded by the Jackson School of Geoscience Recruiting Fellowship and the National Science Foundation Graduate Research
522 Fellowship.

523 **References**

524 Alford, J. J. and Holmes, J. C.: Meander Scars as Evidence of Major Climate Change in Southwest Louisiana, *Ann. Assoc.*
525 *Am. Geogr.*, 75(3), 395–403, doi:10.1111/j.1467-8306.1985.tb00074.x, 1985.
526 Anderson, J. B., Wallace, D. J., Simms, A. R., Rodriguez, A. B. and Milliken, K. T.: Variable response of coastal environments
527 of the northwestern Gulf of Mexico to sea-level rise and climate change: Implications for future change, *Mar. Geol.*, 352, 348–
528 366, doi:10.1016/j.margeo.2013.12.008, 2014.
529 Anderson, J. B., Wallace, D. J., Simms, A. R., Rodriguez, A. B., Weight, R. W. R. and Taha, Z. P.: Recycling sediments
530 between source and sink during a eustatic cycle: Systems of late Quaternary northwestern Gulf of Mexico Basin, *Earth-Science*
531 *Rev.*, 153, 111–138, doi:10.1016/j.earscirev.2015.10.014, 2016.
532 Baker, E. T. J.: Stratigraphic Nomenclature and Geologic Sections of the Gulf, U.S. Geol. Surv. Open-File Rep., 94–461, 34,
533 1995.

534 Bernard, H. A.: Quaternary Geology of Southeast Texas, LSU Historical Dissertations and Theses 7952., 1950.

535 Blom, A., Arkesteijn, L., Chavarrías, V. and Viparelli, E.: The equilibrium alluvial river under variable flow and its channel-
536 forming discharge, *J. Geophys. Res. Earth Surf.*, 122(10), 1924–1948, doi:10.1002/2017JF004213, 2017.

537 Blum, M., Martin, J., Milliken, K. and Garvin, M.: Paleovalley systems: Insights from Quaternary analogs and experiments,
538 *Earth-Science Rev.*, 116(1), 128–169, doi:10.1016/j.earscirev.2012.09.003, 2013.

539 Blum, M. D. and Aslan, A.: Signatures of climate vs. sea-level change within incised valley-fill successions: Quaternary
540 examples from the Texas GULF Coast, *Sediment. Geol.*, 190(1–4), 177–211, doi:10.1016/j.sedgeo.2006.05.024, 2006.

541 Blum, M. D. and Törnqvist, T. E.: Fluvial responses to climate and sea-level change: A review and look forward,
542 *Sedimentology*, 47(SUPPL. 1), 2–48, doi:10.1046/j.1365-3091.2000.00008.x, 2000.

543 Blum, M. D., Morton, R. A. and Durbin, J. M.: “Deweyville” Terraces and Deposits of the Texas Gulf Coastal Plain, *GCAGS*
544 *Trans.*, 45(1950), 53–60, 1995.

545 Bull, W. B.: Stream-terrace genesis: implications for soil development, *Geomorphology*, 3(3–4), 351–367, doi:10.1016/0169-
546 555X(90)90011-E, 1990.

547 Church, M.: Bed Material Transport and the Morphology of Alluvial River Channels, *Annu. Rev. Earth Planet. Sci.*, 34(1),
548 325–354, doi:10.1146/annurev.earth.33.092203.122721, 2006.

549 Daley, J. and Cohen, T.: Climatically-Controlled River Terraces in Eastern Australia, *Quaternary*, 1(3), 23,
550 doi:10.3390/quat1030023, 2018.

551 Erkens, G., Dambeck, R., Volleberg, K. P., Bouman, M. T. I. J., Bos, J. A. A., Cohen, K. M., Wallinga, J. and Hoek, W. Z.:
552 Fluvial terrace formation in the northern Upper Rhine Graben during the last 20 000 years as a result of allogenic controls and
553 autogenic evolution, *Geomorphology*, 103(3), 476–495, doi:10.1016/j.geomorph.2008.07.021, 2009.

554 FEMA: FEMA 2011 1m Liberty Lidar, 2011.

555 Finnegan, N. J. and Dietrich, W. E.: Episodic bedrock strath terrace formation due to meander migration and cutoff, *Geology*,
556 39(2), 143–146, doi:10.1130/G31716.1, 2011.

557 Gagliano, S. M. and Thom, B. G.: Deweyville Terrace, Gulf and Atlantic Coasts. Technical Report 39., Baton Rouge., 1967.

558 Galloway, W. E., Ganey-Curry, P. E., Li, X. and Buffler, R. T.: Cenozoic depositional history of the Gulf of Mexico basin,
559 *Am. Assoc. Pet. Geol. Bull.*, 84(11), 1743–1774, doi:10.1306/8626C37F-173B-11D7-8645000102C1865D, 2000.

560 Garvin, M. G.: Late Quaternary geochronologic, stratigraphic, and sedimentologic framework of the Trinity River incised
561 valley: East Texas coast, , (December), 2008.

562 Guerit, L., Foreman, B. Z., Chen, C., Paola, C. and Castellort, S.: Autogenic delta progradation during sea-level rise within
563 incised valleys, *Geology*, XX(Xx), 1–5, doi:10.1130/g47976.1, 2020.

564 Hancock, G. S. and Anderson, R. S.: Numerical modelling of fluvial strath terrace formation in response to oscillating climate,
565 *Geol. Soc. Am. Bull.*, 114(9), 1131–1142, doi:10.1130/0016-7606(2002)114<1131, 2002.

566 Heinrich, P., Miner, M., Paulsell, R. and McCulloh, R.: Response of Late Quaternary Valley systems to Holocene sea level
567 rise on continental shelf offshore Louisiana: preservation potential of paleolandscapes, , (February), 104, 2020.

568 Hidy, A. J., Gosse, J. C., Blum, M. D. and Gibling, M. R.: Glacial-interglacial variation in denudation rates from interior
569 Texas, USA, established with cosmogenic nuclides, *Earth Planet. Sci. Lett.*, 390, 209–221, doi:10.1016/j.epsl.2014.01.011,
570 2014.

571 Howard, A. D.: Thresholds in river regimes, in *Thresholds in geomorphology*, pp. 227–258., 1980.

572 Ibarra, D. E., Oster, J. L., Winnick, M. J., Rugenstein, J. K. C., Byrne, M. P. and Chamberlain, C. P.: Warm and cold wet states
573 in the western United States during the Pliocene-Pleistocene, *Geology*, 46(4), 355–358, doi:10.1130/G39962.1, 2018.

574 Knox, J. C.: Responses of floods to Holocene climatic change in the upper Mississippi Valley, *Quat. Res.*, 23(3), 287–300,
575 doi:10.1016/0033-5894(85)90036-5, 1985.

576 Lane, E. W.: Design of Stable Channels, *Trans. Am. Soc. Civ. Eng.*, 120(1), 1234–1260, doi:10.1061/TACEAT.0007188,
577 1955.

578 Leigh, D. S.: Late Quaternary climates and river channels of the Atlantic Coastal Plain, Southeastern USA, *Geomorphology*,
579 101(1–2), 90–108, doi:10.1016/j.geomorph.2008.05.024, 2008.

580 Leigh, D. S. and Feeney, T. P.: Paleochannels indicating wet climate and lack of response to lower sea level, southeast Georgia,
581 *Geology*, 23(8), 687–690, doi:10.1130/0091-7613(1995)023<0687:PIWCAL>2.3.CO;2, 1995.

582 Leigh, D. S., Srivastava, P. and Brook, G. A.: Late Pleistocene braided rivers of the Atlantic Coastal Plain, USA, *Quat. Sci.*
583 *Rev.*, 23(1–2), 65–84, doi:10.1016/S0277-3791(03)00221-X, 2004.

584 Lewin, J. and Macklin, M. G.: Preservation potential for late quaternary river alluvium, *J. Quat. Sci.*, 18(2), 107–120,
585 doi:10.1002/jqs.738, 2003.

586 Limaye, A. B. S. and Lamb, M. P.: Numerical simulations of bedrock valley evolution by meandering rivers with variable
587 bank material, *J. Geophys. Res. Earth Surf.*, 119(4), 927–950, doi:10.1002/2013JF002997, 2014.

588 Limaye, A. B. S. and Lamb, M. P.: Numerical model predictions of autogenic fluvial terraces and comparison to climate
589 change expectations, *J. Geophys. Res. Earth Surf.*, 121(3), 512–544, doi:10.1002/2014JF003392, 2016.

590 Mackey, B. H., Roering, J. J. and Lamb, M. P.: Landslide-dammed paleolake perturbs marine sedimentation and drives genetic
591 change in anadromous fish, *Proc. Natl. Acad. Sci. U. S. A.*, 108(47), 18905–18909, doi:10.1073/pnas.1110445108, 2011.

592 Malatesta, L. C., Prancevic, J. P. and Avouac, J. P.: Autogenic entrenchment patterns and terraces due to coupling with lateral
593 erosion in incising alluvial channels, *J. Geophys. Res. Earth Surf.*, 122(1), 335–355, doi:10.1002/2015JF003797, 2017.

594 McGee, D., Moreno-Chamarro, E., Marshall, J. and Galbraith, E. D.: Western U.S. lake expansions during Heinrich stadials
595 linked to Pacific Hadley circulation, *Sci. Adv.*, 4(11), 1–11, doi:10.1126/sciadv.aav0118, 2018.

596 Merritts, D. J., Vincent, K. R. and Wohl, E. E.: Long river profiles, tectonism, and eustasy: A guide to interpreting fluvial
597 terraces, *J. Geophys. Res. Solid Earth*, 99(B7), 14031–14050, doi:10.1029/94JB00857, 1994.

598 Molnar, P., Brown, E. T., Burchfiel, B. C., Deng, Q., Feng, X., Li, J., Raisbeck, G. M., Shi, J., Zhangming, W., Yiou, F. and
599 You, H.: Quaternary Climate Change and the Formation of River Terraces across Growing Anticlines on the North Flank of
600 the Tien Shan, China, *J. Geol.*, 102(5), 583–602, doi:10.1086/629700, 1994.

601 Morton, R. A., Blum, M. D. and White, W. A.: Valley Fills of Incised Coastal Plain Rivers, Southeastern Texas, Gulf Coast

602 Assoc. Geol. Soc., 46, 321–331, doi:10.1306/2DC40B2D-0E47-11D7-8643000102C1865D, 1996.

603 Muto, T. and Steel, R. J.: Autogenic response of fluvial deltas to steady sea-level fall: Implications from flume-tank
604 experiments, *Geology*, 32(5), 401–404, doi:10.1130/G20269.1, 2004.

605 Parker, G., Paola, C., Whipple, K. X. and Mohrig, D.: Alluvial Fans Formed by Channelized Fluvial and Sheet Flow. I: Theory,
606 *J. Hydraul. Eng.*, 124(10), 985–995, doi:10.1061/(ASCE)0733-9429(1998)124:10(985), 1998a.

607 Parker, G., Paola, C., Whipple, K. X. and Mohrig, D.: Alluvial Fans Formed by Channelized Fluvial and Sheet Flow. I: Theory,
608 *J. Hydraul. Eng.*, 124(10), 985–995, doi:10.1061/(ASCE)0733-9429(1998)124:10(985), 1998b.

609 Pazzaglia, F. J.: Fluvial Terraces, in *Treatise on Geomorphology*, vol. 9, pp. 379–412., 2013.

610 Pazzaglia, F. J. and Gardner, T. W.: Fluvial terraces of the lower Susquehanna River, *Geomorphology*, 8(2–3), 83–113,
611 doi:10.1016/0169-555X(93)90031-V, 1993.

612 Pazzaglia, F. J., Gardner, T. W. and Merritts, D. J.: Bedrock fluvial incision and longitudinal profile development over geologic
613 time scales determined by fluvial terraces, pp. 207–235., 1998.

614 Roberts, W. H. G., Valdes, P. J. and Payne, A. J.: Topography’s crucial role in Heinrich Events, *Proc. Natl. Acad. Sci. U. S.*
615 *A.*, 111(47), 16688–16693, doi:10.1073/pnas.1414882111, 2014.

616 Rodriguez, A. B., Anderson, J. B. and Simms, A. R.: Terrace Inundation as an Autocyclic Mechanism for Parasequence
617 Formation: Galveston Estuary, Texas, U.S.A., *J. Sediment. Res.*, 75(4), 608–620, doi:10.2110/jsr.2005.050, 2005.

618 Saucier, R. T.: *Geomorphology and Quaternary Geologic History of the Lower Mississippi Valley*, US Army Corps Eng., I,
619 1–414, 1994.

620 Saucier, R. T. and Fleetwood, A. R.: Origin and Chronologic Significance of Late Quaternary Terraces, Ouachita River,
621 Arkansas and Louisiana, *GSA Bull.*, 81(3), 869–890, doi:10.1130/0016-7606(1970)81[869:OACSOL]2.0.CO;2, 1970.

622 Simms, A. R., Anderson, J. B., Milliken, K. T., Taha, Z. P. and Wellner, J. S.: Geomorphology and age of the oxygen isotope
623 stage 2 (last lowstand) sequence boundary on the northwestern Gulf of Mexico continental shelf, *Geol. Soc. Spec. Publ.*, 277,
624 29–46, doi:10.1144/GSL.SP.2007.277.01.03, 2007.

625 Smith, V. B. and Mohrig, D.: Geomorphic signature of a dammed Sandy River: The lower Trinity River downstream of
626 Livingston Dam in Texas, USA, *Geomorphology*, 297, 122–136, doi:10.1016/j.geomorph.2017.09.015, 2017.

627 Spratt, R. M. and Lisiecki, L. E.: A Late Pleistocene sea level stack, *Clim. Past*, 12(4), 1079–1092, doi:10.5194/cp-12-1079-
628 2016, 2016.

629 Strong, N. and Paola, C.: Fluvial Landscapes and Stratigraphy in a Flume, *Sediment. Rec.*, 4(2), 4–8,
630 doi:10.2110/sedred.2006.2.4, 2006.

631 Sylvia, D. A. and Galloway, W. E.: Morphology and stratigraphy of the late Quaternary lower Brazos valley: Implications for
632 paleo-climate, discharge and sediment delivery, *Sediment. Geol.*, 190(1–4), 159–175, doi:10.1016/j.sedgeo.2006.05.023,
633 2006.

634 Thomas, M. A. and Anderson, J. B.: Sea-Level Controls on the Facies Architecture of the Trinity/Sabine Incised-Valley
635 System, Texas Continental Shelf, in *Incised-Valley Systems: Origin and Sedimentary Sequences.*, SEPM Society for

636 Sedimentary Geology., 1994.

637 Tofelde, S., Savi, S., Wickert, A. D., Bufe, A. and Schildgen, T. F.: Alluvial channel response to environmental perturbations:
638 Fill-terrace formation and sediment-signal disruption, *Earth Surf. Dyn.*, 7(2), 609–631, doi:10.5194/esurf-7-609-2019, 2019.

639 Trinity River Authority of Texas: Phase II, Bathymetry and Sediment Collection for Port of Liberty Study., 2017.

640 U.S. Geological Survey: National Water Information System data available on the World Wide Web (USGS Water Data for
641 the Nation), [online] Available from: <https://waterdata.usgs.gov/usa/nwis/uv?08066500>, 2020a.

642 U.S. Geological Survey: National Water Information System data available on the World Wide Web (USGS Water Data for
643 the Nation), [online] Available from: https://waterdata.usgs.gov/nwis/uv?site_no=08067000, 2020b.

644 Wegmann, K. W. and Pazzaglia, F. J.: Holocene strath terraces, climate change, and active tectonics: The Clearwater River
645 basin, Olympic Peninsula, Washington State, *Bull. Geol. Soc. Am.*, 114(6), 731–744, doi:10.1130/0016-
646 7606(2002)114<0731:HSTCCA>2.0.CO;2, 2002.

647 Whipple, K. X.: Implications of sediment-flux-dependent river incision models for landscape evolution, *J. Geophys. Res.*,
648 107(B2), 2039, doi:10.1029/2000JB000044, 2002.

649 Whipple, K. X., Parker, G., Paola, C. and Mohrig, D.: Channel Dynamics, Sediment Transport, and the Slope of Alluvial Fans:
650 Experimental Study, *J. Geol.*, 106(6), 677–694, doi:10.1086/516053, 1998.

651 Wickert, A. D. and Schildgen, T. F.: Long-profile evolution of transport-limited, , 17–43, 2019.

652 Wilkerson, G. V. and Parker, G.: Physical Basis for Quasi-Universal Relationships Describing Bankfull Hydraulic Geometry
653 of Sand-Bed Rivers, *J. Hydraul. Eng.*, 137(7), 739–753, doi:10.1061/(ASCE)HY.1943-7900.0000352, 2011.

654 Womack, W. R. and Schumm, S. A.: Terraces of Douglas Creek, northwestern Colorado: An example of episodic erosion,
655 *Geology*, 5(2), 72–76, doi:10.1130/0091-7613(1977)5<72:TODCNC>2.0.CO;2, 1977.

656 Young, S. C., Ewing, T., Hamlin, S., Baker, E. and Lupton, D.: Final Report Updating the Hydrogeologic Framework for the
657 Northern Portion of the Gulf Coast Aquifer, , 283, 2012.

658